



## Seafloor sediment characterization to improve estimate of organic carbon standing stocks in continental shelves.

Catherine Brenan<sup>1</sup>, Markus Kienast<sup>1</sup>, Vittorio Maselli<sup>2</sup>, Christopher K. Algar<sup>1</sup>, Benjamin Misiuk<sup>1,3,4</sup>, Craig J. Brown<sup>1</sup>

5 <sup>1</sup>Department of Oceanography, Dalhousie University, Halifax, B3H 4R2, Canada

<sup>2</sup>Department of Earth and Environmental Science, Dalhousie University, Halifax, B3H 4R2, Canada

<sup>3</sup>Department of Geography, Memorial University of Newfoundland, St. John's, A1B 3X9, Canada

<sup>4</sup>Department of Earth Sciences, Memorial University of Newfoundland, St. John's, A1B 3X9, Canada

10 *Corresponding Author:* Craig J. Brown (craig.brown@dal.ca)

**Abstract.** Continental shelf sediments contain some of the largest stocks of organic carbon (OC) on Earth and play a vital role in influencing the global carbon cycle. Quantifying how much OC is stored in shelf sediments and determining its residence time is key to assessing how human activities can accelerate the process of OC remineralization into carbon dioxide. Spatial variations in terrestrial carbon stocks are well studied and mapped at high resolution, but our knowledge of the distribution of marine OC in different seafloor settings is still very limited, particularly in the highly dynamic and spatially variable shelf environments. The lack of knowledge reduces our ability to understand and predict how much and for how long oceans sequester CO<sub>2</sub>. In this study, we use high-resolution multibeam echosounder (MBES) data from the Eastern Shore Islands offshore Nova Scotia (Canada), combined with OC measurements from discrete samples, to assess the distribution of OC content in seafloor sediments. We derive three different spatial estimates of organic carbon: i) assuming a homogenous seafloor the carbon stock estimates were scaled to the entire study region; ii) using a high-resolution substrate map, the estimates were scaled to the areas of soft substrate only, and, finally, iii) using Empirical Bayesian Regression Kriging (EBRK) regression prediction within the area of soft substrate, carbon stock estimates in areas of soft substrate were refined to account for spatial variability in the concentration of OC. These three distinct spatial models yielded dramatically different estimates of average standing stock of OC in our study area, 1275, 259 and 203 Mt of OC respectively. Our study demonstrates that high-resolution mapping is critically important for improved estimates of OC stocks on continental shelves, and to the identification of carbon hotspots that need to be considered in seabed management and climate mitigation strategies.



## 30 1 Introduction

### 1.1 Marine Carbon

Carbon stored and captured in ocean ecosystems is known as blue carbon, and the global ocean can store disproportionate amounts of organic carbon compared to terrestrial carbon stocks (Hilmi et al., 2021). The Intergovernmental Panel on Climate Change (IPCC) define blue carbon as: “*All biologically driven carbon fluxes and storage in marine systems that are amenable to management.*” (Hilmi et al., 2021). Blue carbon is therefore often associated with vegetation in coastal zones, such as tidal marshes, mangroves, and seagrasses (Brown et al., 2016; Fourqurean et al., 2012). Marine sediments are often not included in Blue Carbon calculations and definitions since they do not sequester carbon via photosynthesis (Hunt et al., 2021). However, marine sediments are essential carbon reservoirs and regulate climate change by effectively burying organic carbon over thousands to millions of years if left undisturbed (Avelar et al., 2017; Fennel et al., 2019; Atwood et al., 2020).

Recent studies have concluded that fishing activities such as bottom trawling and dredging can disturb the seafloor with an estimated 1.47 Pg of aqueous CO<sub>2</sub> emissions (Sala et al., 2021). These estimates have substantial errors (Epstein et al., 2022) and often ignore that the mineralization of benthic carbon stores comes from natural cycles (Hilborn et al., 2023). These studies emphasize that further understanding of sediment ocean carbon processes are urgently required to determine if anthropogenic activities could cause the semi-permanent OC stocks in surficial marine sediments to remineralize back to CO<sub>2</sub> (Bianchi et al., 2023). Also, further studies into new approaches to determining the distribution of OC are essential to locate areas of carbon-rich seabed that could become Marine Protected Areas (MPAs).

### 1.2 Seafloor Substrate and Benthic Carbon Mapping

Multibeam-echosounder (MBES) systems provide information about the environmental characteristics of the seafloor, such as depth, hardness, and sediment characteristics, by collecting bathymetry and backscatter information, which can be used to determine seafloor morphology and as a proxy for seafloor substrate type (Brown et al., 2011). Advancements in MBES have allowed us to create spatially continuous high-resolution maps of the ocean floor (Brown et al., 2011; Buhl-Mortensen et al., 2021; Misiuk and Brown, 2023), at a horizontal resolutions down to sub-meter scales (depending on water depth and sonar specifications) (Mayer et al., 2018). Seafloor sediment mapping is defined as using geophysical and sampling systems to determine the character of the surface sediments and includes mapping the quantities of clay/silt, sand, gravel, cobble, and boulder (Misiuk et al., 2019). The modern methods for producing seabed sediment maps combine high-resolution MBES with ground-truth sampling data using machine learning algorithms (Misiuk et al., 2019). Statistical learning techniques include k-Nearest Neighbour (Lucieer et al., 2013; Stephen and Diesing, 2014), Artificial Neural Networks (Huang et al., 2012; Stephen and Diesing, 2014), and Bayesian Decision Rules (Simons and Snellen, 2009; Stephen and Diesing, 2014). The most widely used statistical model for substrate classification and regression maps is Random Forest, due to its ease of implementation and a robust capacity for handling complex, non-linear relationships between environmental variables and ground truthing while avoiding overfitting (Stephen and Diesing, 2015; Misiuk and Brown, 2023).



65 Early carbon mapping studies have applied interpolation methods comprising semi-variogram analyses and kriging to  
spatially predict OC in surficial sediments (Mollenhauer et al., 2004; Acharya and Panigrahi, 2016). More recently,  
soil organic carbon has been modeled using multiple methods in terrestrial ecosystems. Mallik et al. (2022) compared  
artificial neural networks (ANN), Empirical Bayesian Regression Kriging (EBRK), and hybrid approaches combining  
the two, including ANN-OK (ordinary kriging) and ANN-CK (cokriging). They found that the EBRK method  
70 outperformed all other models with highest values of  $R^2$  (0.936) (Mallik et al., 2022). The EBRK method has been  
widely used in terrestrial soil carbon models but has still not been explored for marine sediment carbon models. More  
recent studies have utilized MBES and machine learning algorithms to model and map organic carbon at broad spatial  
scales at the seafloor (Atwood et al., 2020; Diesing et al., 2017; Smeaton et al., 2019). Diesing et al (2017) used  
Random Forest to model particulate organic carbon (POC) at the seafloor using POC measurements from physical  
75 seafloor samples, and spatially continuous seafloor environmental variables (500 m grid resolution) covering the  
Northwest European continental shelf. Similarly, Smeaton et al. (2019) generated a map of seafloor substrate using  
the folk classification and calculated the OC stock per substrate class (100 m grid resolution) (Smeaton et al., 2019).  
Epstein et al. (2023) also used Random Forest to model organic carbon stocks and accumulation rates in surficial  
sediments of the Canadian continental margin at coarse resolution (200m grid resolution) and point out that ignoring  
80 the geographic extent of hard substrate (i.e. bedrock) at these broad spatial scales could inflate carbon stock estimates.  
These studies have been critical to understanding the carbon hotspots at broad spatial scales, as the traditional lower-  
resolution maps often lead to oversimplification and inconsistency in carbon averaging. However, understanding  
distributions of sedimentary OC at a higher spatial resolutions are required for effective seabed management strategies  
(Legge et al., 2020), and .

85 High-resolution maps (6 m grid resolution) of OC have been produced at a local scale using backscatter from MBES  
surveys as a predictor (Hunt et al., 2020; Hunt et al., 2021). Backscatter was determined to be a proxy for OC due to  
extrapolating empirical relationships between sediment grain size and OC (Hunt et al., 2020) and between sedimentary  
properties and backscatter reflectance. This method could be practical in studies where there are scarce sediment data.  
Hunt et al. indicated that the backscatter data reliably captured information regarding the spatial heterogeneity of the  
90 seabed, and that OC correlated strongly with the MBES backscatter signal as a function of sediment composition.  
However, a more recent study suggested that backscatter distinguishes between coarse and fine sediments (low and  
high OC) but struggled to differentiate fine-scale variability within finer-grained sediments (Hunt et al., 2021).

The studies in the North-West European continental margin (Diesing et al., 2017, 2021; Hunt et al., 2020; Hunt et al.,  
2021; Legge et al., 2020; Smeaton et al., 2021) have shown promising early results. Other studies of carbon stocks  
95 have been conducted in the North American Coastal region but without spatially explicit estimates (Fennel et al., 2019;  
Najjar et al., 2018). Overall, spatially mapping OC at the seabed has only been attempted at a few locations globally,  
and there is an urgent need to establish robust approaches to conducting spatial estimates of OC at the seafloor in a  
wide variety of oceanographic setting to improve global estimates of seafloor OC stocks and to help advance our  
understanding of OC fluxes at the seabed (Bianchi et al, 2021, 2023). Our study region, the Eastern Shore islands, is



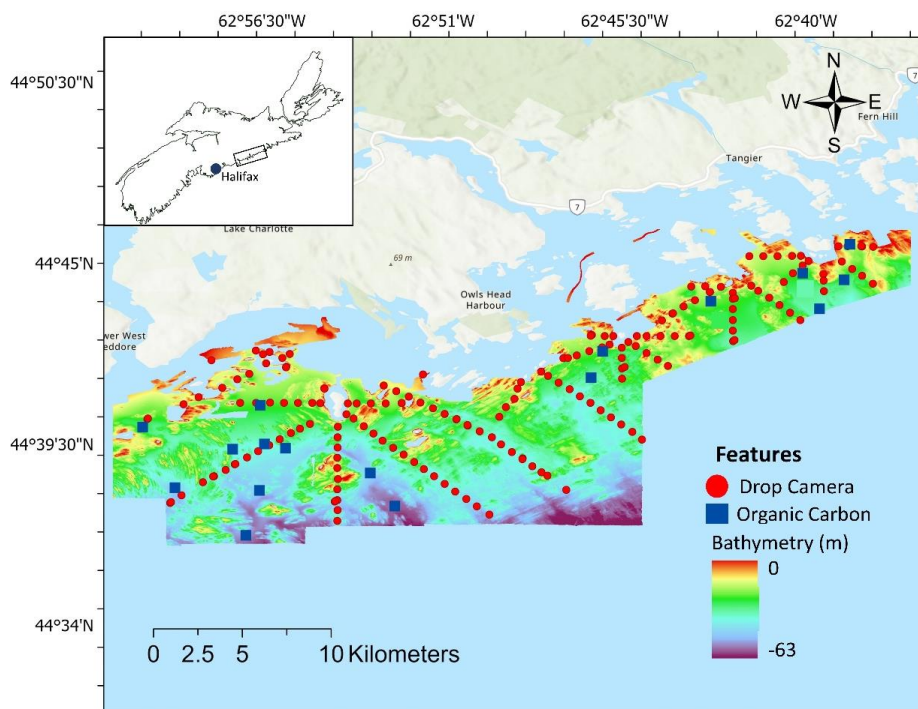
100 an ideal location since it is an Area of Interest for the Canadian government and a heterogeneous seabed, which can provide insight on baseline estimates of sediment organic carbon in complex seafloor types.

This study addresses three key questions:

- 105
- What is the spatial distribution of seafloor sediment types in the Eastern Shore Islands area?
  - Are seafloor sediments a good high-resolution proxy that enable more accurate estimation of organic carbon stocks?
  - Does the spatial heterogeneity of substrate type and carbon content influence estimates of carbon stock?

## 110 2 Study Area

The study region is located within the Eastern Shore Islands (ESI), an area of interest (AOI) for conservation objectives, approximately 60 km northeast of Halifax (Nova Scotia, Canada, Figure 1). The site stretches from Lower West Jeddore to Fern Hill and extends approximately 25 km from the mainland in the Scotian Shelf region with an area of approximately 223 km<sup>2</sup> (Jeffery, 2020).



115



**Figure 1. Seafloor MBES bathymetry outlining the geographical extent for the survey area within the Eastern Shore Islands on the east coast of Nova Scotia, Canada. The drop camera imagery is signified by red points and the blue points are the organic carbon samples. The inset map shows the location in the context of Nova Scotia. (Basemap: Esri NASA, NGA, USGS, Province of Nova Scotia Esri Canada, Esri HERE, Garmin, SafeGraph, METI/NASA, USGS, NRCan, Parks Canada)**

The study area has a water depth between 31 and 63 m. The seafloor is characterized by bedrock, at places covered by a layer of sediments of varying grain size (from clay to boulders) and thickness (King, 2018). Ocean surface temperatures in the ESI are around 1° C in winter for the 0–100 m depth range and increase in the summer with some stratification leading to surface temperatures exceeding 15° C (Jeffery, 2020). By the fall, mixing deepens this warm layer. Ocean currents run predominantly southwestwards on the ESI, with some fluctuation around the coast (Feng et al., 2022). The combination of upwelling, currents, and wind allows for the mixing of nutrients, acting as an essential component of the marine food web in the region (Jeffery, 2020). Nutrients are derived from river, coastal runoff and mixing. They are depleted in the spring due to phytoplankton blooms and replenished in the fall when upwelling is predominant (Jeffery, 2020). Major anthropocentric activities in this area include lobster fishing, recreational fishing, and boating, but the human impact is low due to low population density and coastal development compared to Halifax and St Margaret's Bay (Jeffery, 2020).

### 3 Materials and Methods

#### 3.1 Hydrographic data sets

MBES data were collected by the Canadian Hydrographic Service over two separate surveys (20 June – 29 July 2019; 17 August – 05 September 2020) (Bondt, 2019; Bondt, 2020). Three launches were used to complete this survey – the *CSL Kestrel*, *CSL Tern* and *CSL Pelican*. The survey launch *CSL Kestrel* was equipped with an R2Sonic 2022 multibeam echosounder. The survey launches *CLS Tern* and *CSL Pelican* were outfitted with Kongsberg EM2040C and EM2040C Dual Head echo sounders respectively. All surveys were conducted at MBES operating frequencies of 200-400kHz. Vessel position and orientation were corrected in real time by Trimble/Appplanix POSMV V5 motion compensation systems. Echosounder data was corrected for sound velocity in real time using Applied Microsystems Limited sound velocity sensors. The vessel position was recorded in real-time using the CANNET RTK NTRIP connected directly through the POSMV. Raw position and orientation data from the POSMV were logged throughout the survey for further post-processing where required. Bathymetry and backscatter data were processed using the QPS software suite. Bathymetry data were processed in QIMERA 2.5.3 to generate a bathymetric digital elevation model (DEM) for the survey area. Backscatter data were processed in FMGT 7.10.2 to generate backscatter mosaics for each of the data sets. Backscatter data were not calibrated; the different survey data sets were harmonised using bulk shift methods (Misiuk et al., 2020, 2021; Haar et al, 2023) from areas of overlap between the survey data sets to generate a corrected backscatter mosaic for the entire study area.

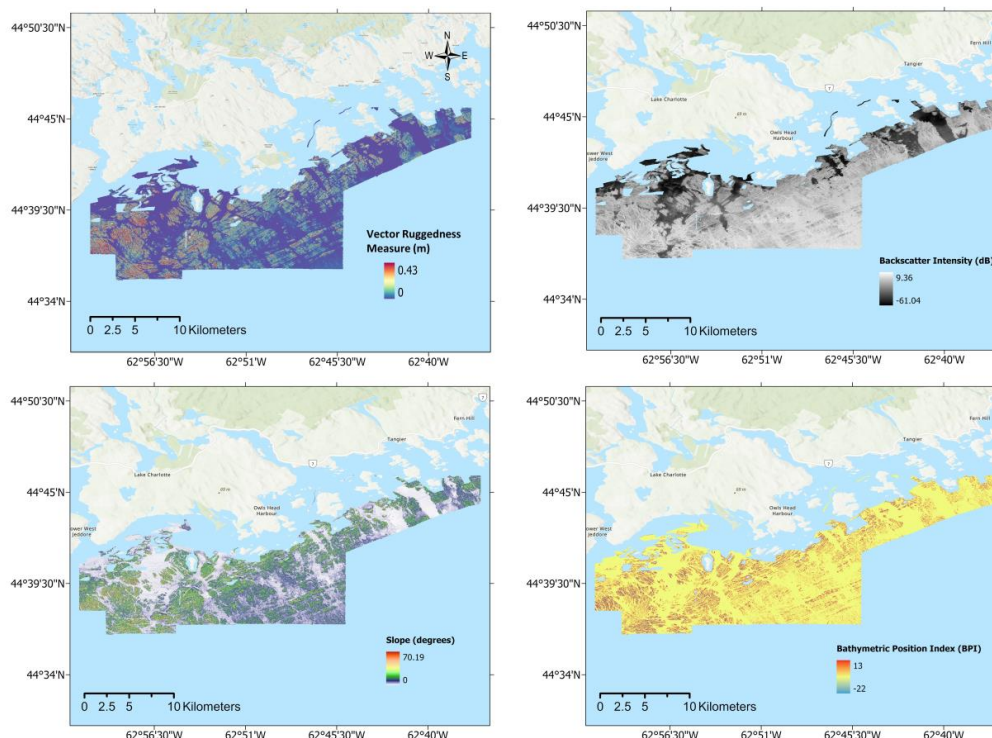
Seafloor morphology features were derived from the primary bathymetric datasets to provide additional predictor variables for the sediment modelling. These were calculated using ArcGIS Pro 3.1.2 and the Benthic Terrain



Modeler (BTM) 3.0 Toolbox. The terrain features included slope, bathymetric position index (BPI) and vector ruggedness measure (VRM), which are considered successful predictors in previous substrate classification studies (Stephen and Diesing, 2015; Misiuk et al, 2019) (Table 1) (Figure 2). The Focal statistics tool was used for all the predictor variables to smooth the surface and reduce noise. These predictor variables were used in both the substrate map and the organic carbon model. The environmental variables were determined based on literature review, expert suggestions, and access to data.

**Table 1. Description of predictor variables used to model sediment type, including their units and description.**

Environmental Variables	Description	Resolution	Units
Bathymetry	Depth	2 m	meters
Backscatter	Measure of intensity of acoustic signal from MBES and indicator of bottom hardness	2 m	relative dB
Slope	Measures maximum change in elevation (steepness)	2 m	degrees
Vector Ruggedness Measure (VRM)	Measures terrain ruggedness of grid cells within a neighbourhood	2 m	meters
Broad Bathymetric Position Index (BPI)	Differences in values of centre cell to mean of surrounding cells.	2 m	meters



160

**Figure 2. Backscatter, Slope, VRM and BPI data mapped in the Eastern Shore Islands study area. (Basemaps: Esri NASA, NGA, USGS, Province of Nova Scotia Esri Canada, Esri HERE, Garmin, SafeGraph, METI/NASA, USGS, NRCan, Parks Canada)**

### 165 **3.2 Seabed sediment sampling**

Sampling surveys for OC and grain size were conducted between 9 - 27 May 2022 from the *MV Island Venture*. A stratified random sampling technique was used based on the backscatter mosaic (Figure 2). Acoustic backscatter was used to select sampling locations since it is a good proxy of sediment grain size and is commonly used in substrate classification routines (Hunt et al., 2020). A Van Veen grab sampler fitted with a GoPro camera was operated to collect sediment samples and drop camera imagery at each sample location, with the grab penetrating up to 10 cm depth into the substrate. The GPS position of the research vessel was recorded at the point of contact on the seabed at each grab station. Grab deployments were done only in areas of soft substrate where it was possible to retrieve a sample. Generally, it is difficult to sample a coarser sediment matrix successfully, and these sediment types are often under-represented in sedimentary carbon studies (Hunt et al., 2020). After thoroughly mixing the sediment in the Van Veen grab, subsamples of sediment were taken from the grabs and placed in a 32 oz plastic container for organic carbon analysis. Following collection, these samples were stored in a cooler during the day and put into a freezer in the evening.

170

175



### 3.3 Processing of sediment grab samples

The sedimentary OC from the grab samples was quantified using an elemental analyzer (Elementar microcube) with a detection limit of 0.03 mg. Based on the method from Verardo et al. (1990), samples were dried in the oven at 60° C overnight and ground using a mortar and pestle to form a homogenous powder. Coarse-grained sediments (above 2 mm diameter) were excluded since they are too large for elemental analysis. Two samples (ES-31, ES-35) had notable amounts of course-grained sediments (around 30% of sample). The coarse fraction was removed from these samples, and the % OC adjusted accordingly. Silver capsules were used to weigh the initial mass (0.5-0.7 mg), and acid fumigation was performed by exposing the samples to 37% hydrochloric acid (HCl) to remove any IC. It is significant to note that an acid wash could also potentially remove some OC, which could alter the results (Verardo et al., 1990). These capsules were then placed in an oven overnight at 60° C before undergoing analysis.

Sediment grain size analysis was conducted using the protocol derived from Mason (2011). The sediment was first split into pebble/cobble (>4000 µm), gravel (>2000 µm) and fine sediment (<2000 µm) material using mesh sieves. The fraction <2000 µm was evaluated using a Beckman Coulter's LS 13 320 particle size analyzer at the Bedford Institute of Oceanography. Following guidance by Mason (2011), the samples were not treated with acid or hydrogen peroxide because of the relatively low organic content. The results from the coarse and fine-scale fractions were combined into a full particle size distribution to determine the percentages of the different sediment types (supplementary material).

195

### 3.4 Subsea video surveys

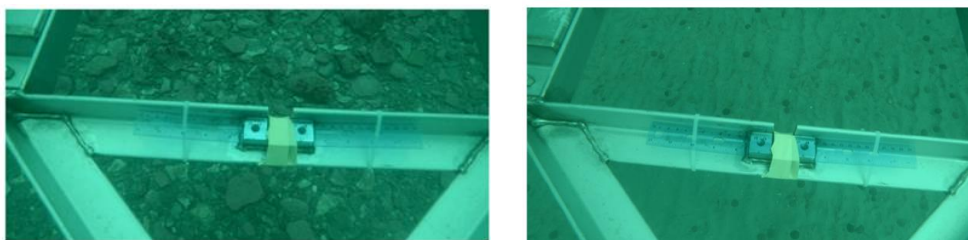
A total of 174 drop camera stations were conducted by Fisheries and Oceans Canada (DFO) over 13 days during September and October 2017 aboard the vessel *RV Sigma-T* (Jeffery et al., 2020) (Figure 1). An HD subsea video camera (SV-HD SDI) which recorded camera positional information using a video overlay (Proteus II), where it received positional and time/date stamp data from the chart plotter (Vandermeulen, 2018). The overlay sent the completed video feed to a direct-to-disk HD recorder and a standard low-power LED TV. The GPS antenna for the navigation system was mounted on the roof of the wheelhouse approximately 10 m distant from the drop camera when deployed off the stern gallows. In this manner, all positional information in the video overlay would be offset by at least 10 m. This offset was accounted for in subsequent analyses. Drop camera targets from the GIS were labelled and embedded into the *RV Sigma-T* navigation computer. Approximately three minutes of video was recorded at each drop camera location with the camera light turned on. All the drop camera sites were at depths greater than 10 m. Additionally, the camera imagery of the seafloor collected from the GoPro camera fitted to the grab sampler during the sampling of organic carbon in 2022 (see sediment sampling section above) was also incorporated with the imagery conducted by DFO for subsequent analysis (Figure 1).





From each video station, a presence (1) and absence (0) of different sediment types were recorded in post processing. The data was classified into two sediment types: Hard substrate (rock, boulder, cobbles, pebbles, and gravel), and soft substrate (mud and sand) (Figure 3) (supplementary material).

215



220 **Figure 3. Example of seafloor imagery from each of the two substrate classes: Hard Substrate (left); soft substrate (right). Photos from a GoPro camera mounted on the van veen grab. Width of images are approximately 0.5 m, with the frame of the grab providing scale for classification of substrata.**

### 3.5 Sediment Modelling

225 Random Forest has been used in previous carbon mapping studies due to its high predictive accuracy, capacity to manage many predictor variables, and unbiased internal validation (Diesing et al., 2017). Random Forest was performed here using R version 4.3.1 with the randomForest package (Liaw and Wiener, 2002). The model was initially trained with default hyperparameters ( $n_{tree} = 500$ ,  $m_{try} = 2$ ,  $nodesize = 1$ ) using the substrate classification observations and all predictor variables (bathymetry, backscatter, BPI, VRM and slope). Random Forest is an ensemble modelling approach comprising many individual classification trees, each grown on a bootstrapped version of the dataset. The observations not selected for a given tree are termed the “out-of-bag” (OOB) observations. Given enough trees, each response observation will be represented in the OOB sample multiple times. By predicting the OOB values for each individual tree during model training, the results can be aggregated over all trees to provide a useful set of validation predictions that have not been exposed to training observations. The OOB observations were used here to estimate predictor variable importance by permuting the predictor values and measuring the resulting increase in OOB error (Liaw and Wiener, 2002). Random Forest is generally considered robust to the use of correlated predictors and estimates of importance additionally suggested contribution to the model by all variables, which were thus retained. Informal trials suggested that a model of 100 trees (i.e.,  $n_{tree} = 100$ ) provided sufficient predictive capacity but improved computational speed. After training the final model with these parameters, a confusion matrix was generated using the OOB observations and predictions to evaluate the map accuracy, and the model was then predicted across the full map extent using the predictor variable rasters.

230  
235  
240



### 3.6 Estimation of Total Standing Stock of Organic Carbon

The elemental analyser reports OC value as a proportion (weight %). Previous studies have stated that an arcsine transformation on the OC value ( $X$ ) is advisable since it can make the variance constant and the data appears normally distributed (Sokal and Rohlf, 1981; Diesing et al., 2017):

$$245 \quad Y = \arcsin\sqrt{X} \quad (1)$$

Dry bulk density was not measured directly in this study but calculated from estimated porosity and density. Porosity ( $\Phi$ ) is calculated from predicted mud content (dimensionless fraction), which is a combination of clay and silt from the grain size distribution measurements using the equation (2) derived from Jenkins (2005).

$$\Phi = 0.3805 * C_{mud} + 0.42071 \quad (2)$$

250  $\Phi$  and  $C_{mud}$  (mud content) are dimensionless fractions. The equation was derived based on data from the Mississippi-Alabama-Florida shelf, and it is assumed that the equation is not site-specific (e.g., Diesing et al., 2017).

Dry bulk density ( $p_d$ ) of the sediment was estimated using the porosity and sand grain density ( $p_s = 2650 \text{ kg m}^{-3}$ ) (Diesing et al., 2017; Hunt et al., 2020):

$$255 \quad p_d = (1 - \Phi) p_s \quad (3)$$

Following prior studies that quantified marine sedimentary organic carbon (e.g., Diesing 2017, Hunt 2021), the standing stock of organic carbon ( $m_{oc}$ ) per grid cell was estimated by multiplying the transformed organic carbon concentration ( $Y$ ), dry bulk density ( $p_d$ ), the average sampling depth of the Van Veen grab ( $d = 0.1 \text{ m}$ ) and area of mapped grid cell ( $A = 4 \text{ m}^2$ ) using the equation (4) below:

$$260 \quad m_{oc} = Y * p_d * d * A \quad (4)$$

### 3.7 Spatial Interpolation of Organic Carbon

The spatial distribution of OC measurements indicated substantial heterogeneity among the soft sediments of the study site. To further refine the estimation of OC in areas of soft sediment, Empirical Bayesian Regression Kriging (EBRK) was used for the spatial interpolation of OC stock ( $m_{oc}$ ) and estimation of values at unknown locations  
265 within the extent of the soft substrate. EBRK is a geostatistical interpolation method that combines ordinary least square regression and kriging to provide accurate predictions of non-stationary data at a local scale (Giustini et al., 2019). An exponential semi-variogram model and an empirical transformation was performed since it provided the lowest error in the cross-validation results. EBRK was performed in the geostatistical wizard in ESRI ArcGIS Pro 3.1. The EBRK model was evaluated using leave-one-out cross-validation (Mallik et al., 2022). The model  
270 was validated according to the mean error (ME) and the root-mean-square error (RMSE). ME is the average of the cross-validation errors, measures model bias and should have a value close to zero (Acharya and Panigrahi,



2016). RMSE is defined as the square root of the average squared prediction errors and measures prediction accuracy. This value should be as small as possible.

## 4 Results

### 275 4.1 Grain size Distributions, Sediment Properties, and Organic Carbon Concentrations

Van Veen grab samples provided grain size and organic carbon measurements at each station (Table 2). It is important to note that silt and clay were merged into a single mud class to estimate the OC stock.

**Table 2. Raw data from grab samples including grain size and organic carbon measurements.**

Station	>4000 um (%)	>2000 um (%)	Sand Content (%)	Clay Content (%)	Silt Content (%)	Porosity	Dry Bulk Density (kg/m <sup>3</sup> )	Organic Carbon (%)
ES-02	0.27	0.08	54.3	7.13	38.4	0.59	1077.6	1.22
ES-03	0.003	0.06	90.8	2.03	7.11	0.46	1443.0	0.12
ES-04	0.33	0.01	93.7	1.69	4.28	0.44	1475.1	0.13
ES-07	0.00	0.00	24.4	10.3	65.2	0.71	773.0	1.85
ES-15	0.59	0.11	94.6	1.29	3.44	0.44	1487.4	0.06
ES-17	2.07	0.30	63.7	4.18	30.5	0.55	1185.1	0.10
ES-18	0.60	0.04	80.2	1.93	17.4	0.49	1340.5	0.23
ES-19	0.00	0.04	96.7	1.12	2.15	0.43	1502.2	0.08
ES-21	0.14	0.10	91.4	1.17	7.23	0.45	1450.4	0.06
ES-23	0.08	0.21	93.8	1.27	4.68	0.44	1475.1	0.07
ES-25	0.006	0.01	95.4	1.05	3.50	0.44	1489.3	0.05
ES-27	0.04	0.05	85.0	1.67	13.3	0.48	1384.7	0.07
ES-28	0.00	0.05	85.2	1.63	13.2	0.48	1385.8	0.08
ES-29	0.00	0.02	86.7	1.87	11.4	0.48	1401.4	0.08
ES-31	21.42	9.97	45.8	4.78	28.5	0.51	1199.2	0.57



ES-34	2.15	0.71	52.4	6.15	39.9	0.59	1071.1	0.61
ES-35	34.00	0.37	17.3	8.83	64.8	0.61	793.01	0.62

280

#### 4.2 Relationship between Grain size and Organic Carbon

An ordinal least square regression (OLS) was performed to examine the relationship between OC and the percentage grain size composition of mud. There was a significant positive relationship between OC and percent mud ( $p < 0.001$ ;  $R^2 = 0.81$ ) (Figure 4), suggesting that, here, sediment type may be useful as a proxy for OC (Burdige, 2007; Hedges & Keil, 1995; C. A. Hunt et al., 2021).

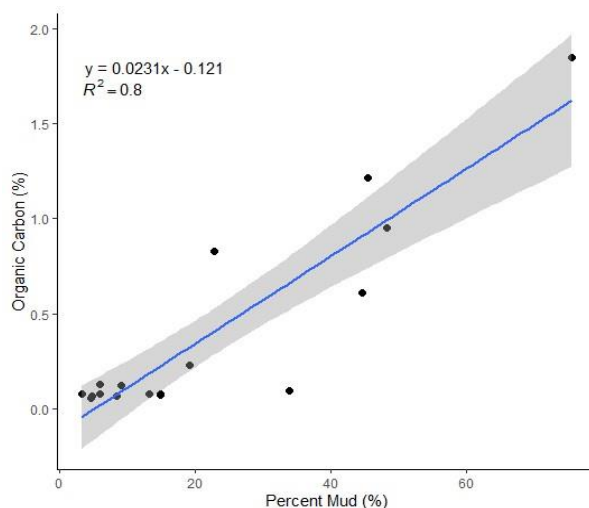
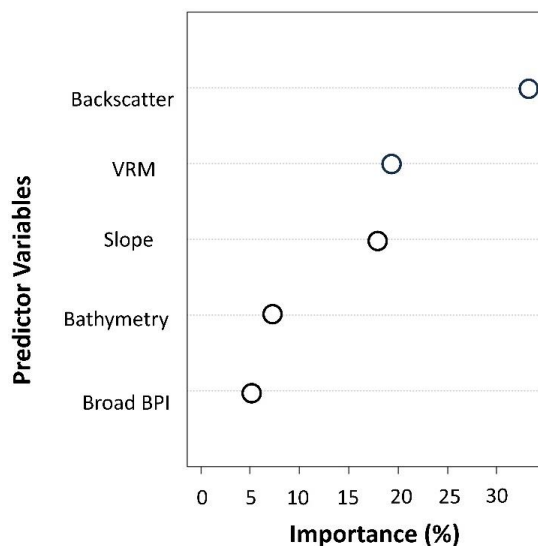


Figure 4. Linear regression indicating the relationship between OC and percent mud (top right). The grey area represents a 95 percent confidence interval for the slope of the regression line.

#### 290 4.3 Substrate Classification Map

Outputs from Random Forest indicated that bathymetry, backscatter, vector ruggedness measure (VRM) and slope were all important for the sediment classification. Figure 5 shows the relative significance of the five variables to prediction accuracy. Backscatter was the most important variable for predicting sediment type, followed by VRM, slope, bathymetry, and BPI.



295

**Figure 5. Variable Importance scores.** The importance of predictor variables as indicated by the Random Forest algorithm. The y axis indicates the variables of the final model, the x-axis indicates the relative percent importance.

The confusion matrix is presented in Table 3. The Kappa score was 0.69 and F1 was 0.91 (Table 4). These statistics indicate that the OOB samples were predicted with high accuracy (87%) and precision (89%), suggesting that the model was able to successfully differentiate soft and hard substrates within the study area.

300

**Table 3. Confusion Matrix of sediment map**

		Actual Values	
		Hard Substrate	Soft Substrate
Predicted Values	Hard Substrate	129	16
	Soft Substrate	9	44

305 **Table 4. Performance of Substrate Model**

Substrate Classification	Kappa	F1-Score	Sensitivity (%)	Accuracy (%)	Specificity (%)	Precision (%)
	0.6909	0.9117	93.48	87.37	73.33	88.97

The sediment classification map revealed that the hard substrate was the most spatially extensive (178 km<sup>2</sup>) whereas the soft substrate class was smaller, covering approximately 45 km<sup>2</sup> of the study area, corresponding with contiguous



patches of relatively low relief seafloor (Figure 6). Sediment grain size revealed average percentiles  $d_{10}=17$   $\mu\text{m}$ ,  $d_{50}=147$   $\mu\text{m}$  and  $d_{90}=1822$   $\mu\text{m}$ . This suggests that most sediment samples were represented by sand, with varying smaller proportions of silt and clay (Figure 7). Two samples were comprised of around 30% gravel ( $>2000$   $\mu\text{m}$ ) (Figure 7).

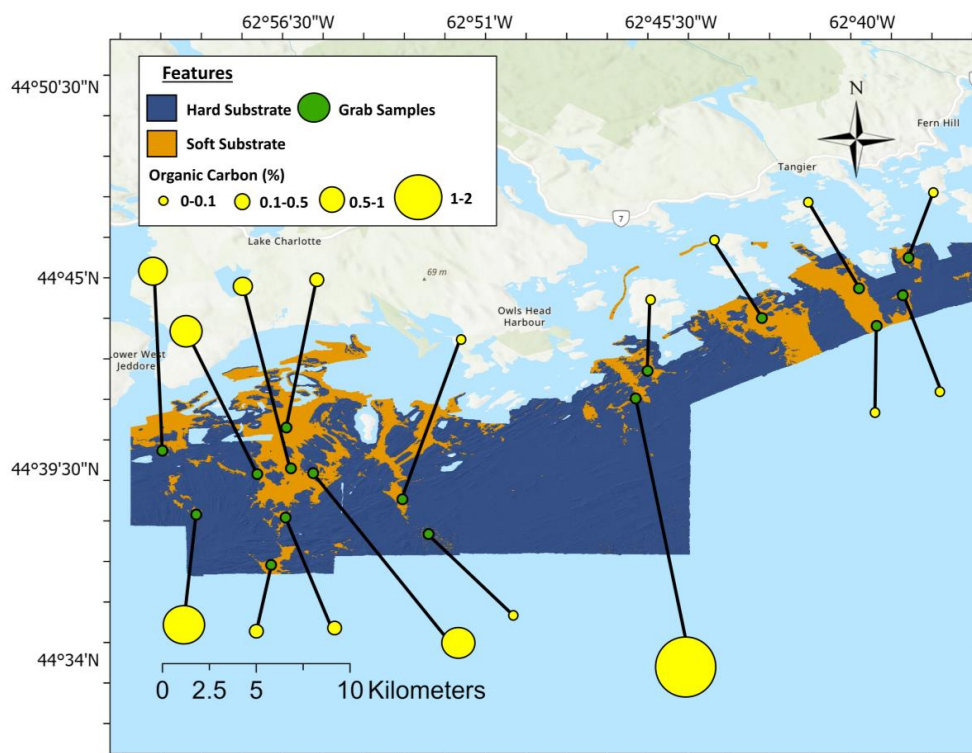
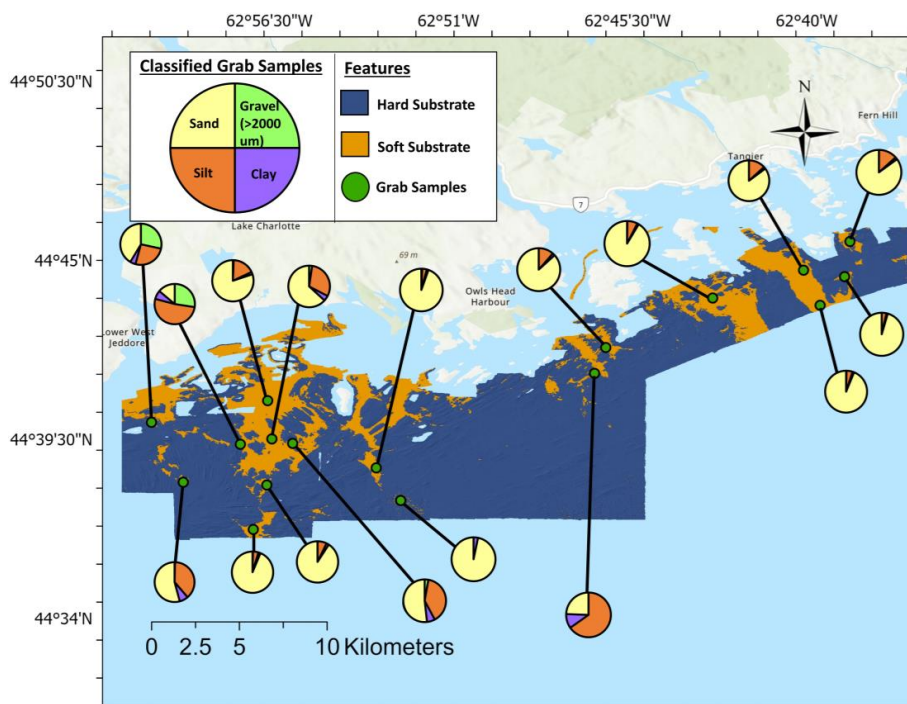


Figure 6. Sediment classification map indicating areas of hard (orange) and soft substrate (blue). Proportional symbols of organic carbon indicate the sampled percentage (yellow). (Basemap: Esri NASA, NGA, USGS, Province of Nova Scotia Esri Canada, Esri HERE, Garmin, SafeGraph, METI/NASA, USGS, NRCan, Parks Canada)



**Figure 7. Sediment classification map indicating predicted hard (orange) and soft substrate (purple). Pie charts depict ratios of sand (yellow), silt (orange red), clay (purple), and gravel (green) found in each sediment sample collected. (Basemap: Esri NASA, NGA, USGS, Province of Nova Scotia Esri Canada, Esri HERE, Garmin, SafeGraph, METI/NASA, USGS, NRCan, Parks Canada)**

#### 4.4 Organic Carbon Prediction

Cross-validation of the EBRK model indicated the accuracy of OC ( $m_{oc}$ ) predictions in the soft sediment areas. Results had ME= 0.16 kg/m<sup>3</sup> and RMSE= 7.93 kg/m<sup>3</sup> (Table 5). These results imply that the model performed a minimal biased prediction and overall accurate interpolation of the organic carbon.

**Table 5. EBRK model details**

No of simulation	Model selected	No of variables	ME	RMSE
100	Exponential	5	0.16	7.93

After calculating the porosity, dry bulk density and measuring percent OC, the predicted mass of OC per unit area ( $m_{oc}$ ) was determined and spatially interpolated. The spatial distribution of  $m_{oc}$  values is shown in Figure 8. The highest amount of OC concentration was found in the west of the study area along with a small patch of high concentration near Owls Head Harbour.

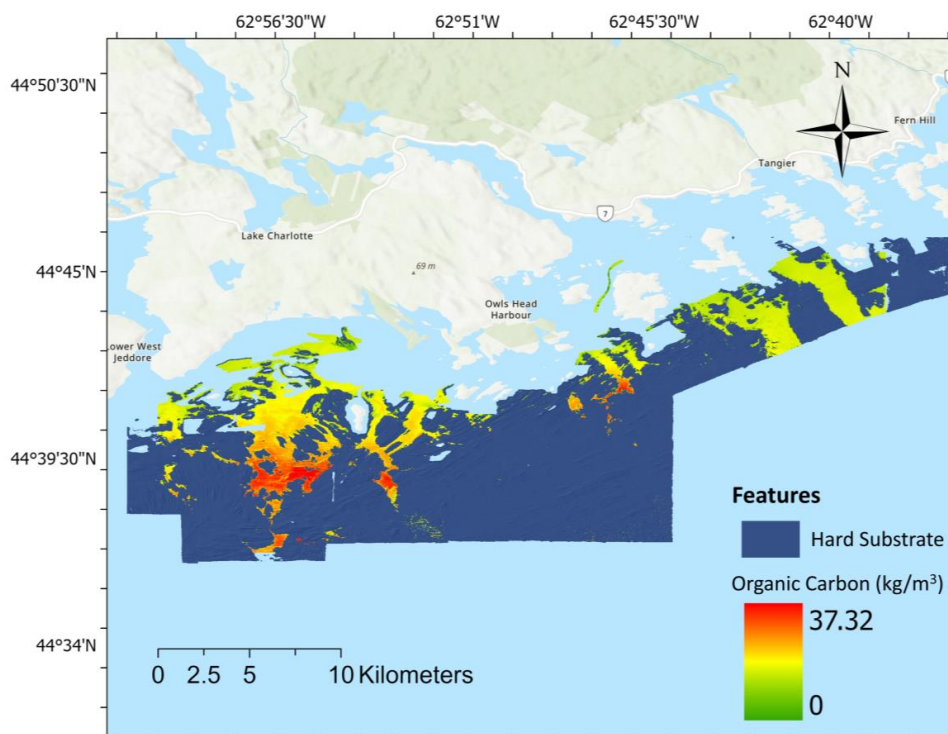


**Figure 8. Spatial interpolation of organic carbon using the EBRK method. Low quantities of organic carbon are represented by green and the high quantities by red. (Basemap: Esri NASA, NGA, USGS, Province of Nova Scotia Esri Canada, Esri HERE, Garmin, SafeGraph, METI/NASA, USGS, NRCan, Parks Canada)**

#### 4.5 Organic Carbon Estimates

Estimates of OC were calculated for three scenarios: 1) assuming a homogeneous seafloor across the study area (i.e. lacking high-resolution seafloor mapping data); 2) averaging OC across the soft sediment area; 3) estimating spatial heterogeneity of OC across the soft sediment area (Table 6) (supplementary material). In scenario 1, the OC samples were scaled up to the entire study area with an average estimate of 1275 Mt. In scenario 2, when using the high-resolution substrate map (assuming negligible OC in the hard substrate regions), the average  $m_{OC}$  for the study area was calculated at 259 Mt. In scenario 3, after determining the average  $m_{OC}$  found in the spatially interpolated soft sediment areas, the quantity was estimated at 203 Mt of OC. The second two estimations assume that there is no OC within the coarse substrata and is based on the spatial extent of the soft substrate class.





350 **Table 6. Calculations used to determine the total stock of OC in the mud/sand sediment type and the total stock of OC in the entire study area.**

Maps	Average Dry Bulk Density (kg/m <sup>3</sup> )	Average organic carbon (%)	Min of OC (%)	Max of OC (%)	Average stock of organic carbon per grid cell (kg/m <sup>3</sup> )	Total grid cells	Total stock of organic carbon in study area (Mt)
Scenario 1: Assuming homogenous seabed	1290.1 ± 237.4	0.35	0.054	1.85	22.85 ± 10.69	5.58E+07	1275 (772 to 2655)
Scenario 2: Soft sediments					1.13E+07		259 (157 to 539)
Scenario 3: EBRK organic carbon map					17.87 ± 4.59	203	

### 5 Discussion

Our study explores how high-resolution spatial models can improve carbon budget estimates. We have described a quantitative spatial model of hard and soft substrate on a continental shelf and determined three estimates of total  $m_{OC}$  in the surficial (top 10 cm) sediments: scaling to the entire study area (scenario 1), the area of soft substrate only (scenario 2), and the refined  $m_{OC}$  within the soft substrate estimated from the EBRK model (scenario 3). The results demonstrate that as spatial models become more detailed, the accuracy of  $m_{OC}$  estimates increases, while the estimates of organic carbon stock decrease substantially.

The sediment map effectively classified the hard and soft substrate ( $F1=0.91$ ) and significantly refined our understanding of the detailed distribution of the organic carbon. Previous studies have applied similar machine learning modelling approaches with success (Stephen and Diesing et al., 2015; Misiuk et al., 2019; Mitchell et al., 2019; Epstein et al. 2023). Our results further demonstrate that this approach is suitable for mapping benthic substrates where high-resolution MBES data sets and suitable sediment ground-truthing are available. Other studies have found that the highest mass of POC was associated with gravelly mud, mud, and sandy mud areas (Diesing et al., 2017). This agrees with our OLS analysis that areas of increased OC have a high mud content (Figure 4). The empirical relationship observed between sediment grain size and OC strongly suggests the importance of using substrate maps to precisely estimate the stock of OC.



385 Differences in estimated OC stock suggest that the substrate map was an essential component to this study. There  
is commonly an assumption in benthic OC studies that the seafloor is homogenous (Smeaton et al., 2021). Since  
shelf environments are inherently heterogeneous, scaling up the approach applied here where high resolution  
mapping data are available offers an effective way of obtaining accurate estimates of OC in shelf environments  
(Snelgrove et al., 2018). To improve estimates and better identify how the ocean carbon cycle will be altered by  
390 climate change, carbon studies should embrace the full complexity of the seafloor (Snelgrove et al., 2018; Epstein  
et al., 2023). Our study also emphasizes the benefits of high resolution MBES data for such applications, and the  
need for additional coverage and collection of seafloor mapping data sets in coastal waters where coverage is  
currently limited (Mayer et al, 2018).

395 The difference in the total  $m_{OC}$  calculated based on the substrate map (259 Mt of OC) versus estimates in the  
absence of a map (1275 Mt of OC) emphasizes that a spatial component to OC estimations is essential for carbon  
system models. This difference demonstrates the need to understand the presence of hard substrate at the seabed  
when calculating carbon stocks as emphasized in recent broadscale carbon modelling studies (Epstein et al., 2023).  
Currently, global carbon models are oversimplifying carbon processes due to our lack of understanding of the  
400 complexity of the marine carbon cycle. For instance, previous studies have examined carbon quantity at the surface  
of the oceans by analyzing phytoplankton activity using satellite imagery, since there is an assumption that carbon  
at the surface of the oceans correlates with areas of high carbon storage at the seafloor (Chase et al., 2022). This  
assumption ignores the complexity of carbon moving through the pelagic and benthic regions. Spatially  
continuous seafloor mapping data is a step towards improving accuracy in our estimation, which will enhance the  
405 ongoing investigations into the marine carbon cycle.

Additionally, the resolution of the seafloor mapping data is an important factor when modeling OC. For instance,  
by using a 2m-by-2m grid resolution we can interpolate the carbon within the soft substrate using EBRK models.  
Through the EBRK interpolation of carbon, the total  $m_{OC}$  (203 Mt of OC) was less than the estimates that assume  
410 a homogenous soft substrate. The EBRK method indicates that high resolution interpolated models of OC can  
help to further refine standing stock estimates and provide insight into where the carbon hotspots are within the  
study area.

### 5.1 Future Implications of OC models

415 Marine spatial planners are trying to manage the seabed in a sustainable manner and high resolution regional-scale  
OC mapping data could be a practical option to help identify vulnerable C stores and hotspots, and to determine  
how these areas may be altered due to environmental change and anthropocentric activities (Hunt et al., 2021).  
Marine protected areas have been defined as regions that conserve marine resources, ecosystem services or cultural  
heritage (Mayr et al., 2010). High-resolution seafloor OC models could help redefine MPAs and allow them to



420 incorporate areas of high carbon sequestration. It is important to recognize sediments as long-term carbon sinks  
that provide climate regulation services.

It is challenging to measure how anthropocentric activities like bottom trawling are impacting the seabed and how  
they influence OC without understanding of the natural processes of marine carbon cycling. Studies that examine  
OC spatially and its connections to seafloor composition are a crucial component to piecing together the natural  
425 marine carbon cycle, which can help determine if the amount of remineralization occurring from human activities  
will have a substantial impact on climate. Even with a relatively limited number of OC samples, this study  
demonstrates that high-resolution seafloor substrate maps and spatial OC models are critical to understanding the  
spatial heterogeneity of organic carbon on the seafloor.

## 6 Conclusions

430 We have presented a method that utilizes high-resolution sedimentary maps and spatial models to quantify OC  
estimates. We show that examining the spatial heterogeneity of carbon content within the soft substrate can improve  
the estimates of organic carbon content. These results emphasize that further research should explore high-resolution  
multibeam echosounder data in determining OC rich hotspots to help support management measures. In this study,  
435 additional ground truthing is necessary to create more precise measurements of OC and to further evaluate which  
sediment type is most significant for OC storage. Despite the limited dataset, high-resolution sediment classification  
maps are necessary to improve our understanding of spatial patterns of OC. Additional surficial sediment OC  
distribution studies are necessary to improve seabed management and marine policy.

## Data Availability

440 Bathymetry data was obtained from the Canadian Hydrographic Service (CHS) NONNA Portal -[https://data.chs-  
shc.ca/login](https://data.chs-shc.ca/login). All other data used in this study is in the supplementary material or available upon reasonable request.

## Competing Interests

One authors is a members of the editorial board of *Biogeosciences*.

445



## References

- 450 Acharya, S. S., & Panigrahi, M. K. (2016). Evaluation of factors controlling the distribution of organic matter and phosphorus in the Eastern Arabian Shelf: A geostatistical reappraisal. *Continental Shelf Research*, 126, 79–88. <https://doi.org/10.1016/j.csr.2016.08.001>
- Atwood, T. B., Witt, A., Mayorga, J., Hammill, E., & Sala, E. (2020). Global Patterns in Marine Sediment Carbon Stocks. *Frontiers in Marine Science*, 7, 165. <https://doi.org/10.3389/fmars.2020.00165>
- 455 Avelar, S., van der Voort, T.S. & Eglinton, T.I. Relevance of carbon stocks of marine sediments for national greenhouse gas inventories of maritime nations. *Carbon Balance Manage* **12**, 10 (2017). <https://doi.org/10.1186/s13021-017-0077-x>
- Bianchi, T.S., Aller, R.C., Atwood, T.B., Brown, C.J., Buatois, L.A., Levin, L.A., Levinton, J.S., Middelburg, J.J., Morrison, E.S., Regnier, P., Shields, M.R., Snelgrove, P.V., Sotka, E.E., & Stanley, R.R. (2021). What global  
460 biogeochemical consequences will marine animal–sediment interactions have during climate change? *Elementa: Science of the Anthropocene* 9: 1. doi.10.1525/elementa.2020.00180
- Bianchi, T. S., Brown, C. J., Snelgrove, P. V. R., Stanley, R. R. E., Cote, D., & Morris, C. (2023). Benthic Invertebrates on the Move: A Tale of Ocean Warming and Sediment Carbon Storage. *Limnology and Oceanography Bulletin*, 32(1), 1–5. <https://doi.org/10.1002/lob.10544>
- 465 Bondt, G. (2019). Final Field report for the Eastern Shore Islands. CHSDIR Project Number: 2901633 1001-07-F01\_2901633\_2602567\_EasternShore\_FFR%20(1).pdf
- Bondt, G. (2020). Final Field report for the Eastern Shore Islands. CHSDIR Project Number: 9000294 9000713\_1001-07-F01\_9000294\_EasternShore\_2020\_Field%20Report%20(1).pdf
- Brown, C. J., Smith, S. J., Lawton, P., & Anderson, J. T. (2011). Benthic habitat mapping: A review of progress towards  
470 improved understanding of the spatial ecology of the seafloor using acoustic techniques. *Estuarine, Coastal and Shelf Science*, 92(3), 502–520. <https://doi.org/10.1016/j.ecss.2011.02.007>
- Brown, D. R., Conrad, S., Akkerman, K., Fairfax, S., Fredericks, J., Hanrio, E., Sanders, L. M., Scott, E., Skillington, A., Tucker, J., Van Santen, M. L., & Sanders, C. J. (2016). Seagrass, mangrove and saltmarsh sedimentary carbon stocks in an urban estuary; Coffs Harbour, Australia. *Regional Studies in Marine Science*, 8, 1–6.  
475 <https://doi.org/10.1016/j.rsma.2016.08.005>



- Buhl-Mortensen, P., Lecours, V., & Brown, C. J. (2021). Editorial: Seafloor Mapping of the Atlantic Ocean. *Frontiers in Marine Science*, 8, 721602. <https://doi.org/10.3389/fmars.2021.721602>
- Burdige, D. J. (2007). Preservation of Organic Matter in Marine Sediments: Controls, Mechanisms, and an Imbalance in Sediment Organic Carbon Budgets? *Chemical Reviews*, 107(2), 467–485. <https://doi.org/10.1021/cr050347q>
- 480
- Chase, A. P., Boss, E. S., Haëntjens, N., Culhane, E., Roesler, C., & Karp-Boss, L. (2022). Plankton Imagery Data Inform Satellite-Based Estimates of Diatom Carbon. *Geophysical Research Letters*, 49(13). <https://doi.org/10.1029/2022GL098076>
- Diesing, M., Kröger, S., Parker, R., Jenkins, C., Mason, C., & Weston, K. (2017). Predicting the standing stock of organic carbon in surface sediments of the North–West European continental shelf. *Biogeochemistry*, 135(1–2), 183–200. <https://doi.org/10.1007/s10533-017-0310-4>
- 485
- Epstein, G., Middelburg, J. J., Hawkins, J. P., Norris, C. R., & Roberts, C. M. (2022). The impact of mobile demersal fishing on carbon storage in seabed sediments. *Global Change Biology*, 28(9), 2875–2894. <https://doi.org/10.1111/gcb.16105>
- 490
- Epstein, G., Fuller, S. D., Hingmire, D., Myers, P. G., Peña, A., Pennelly, C., & Baum, J. K. (2023). Predictive mapping of organic carbon stocks and accumulation rates in surficial sediments of the Canadian continental margin, Earth Syst. Sci. Data Discuss. [preprint], <https://doi.org/10.5194/essd-2023-295>, in review.
- Feng, T., Stanley, R. R. E., Wu, Y., Kenchington, E., Xu, J., & Home, E. (2022). A High-Resolution 3-D Circulation Model in a Complex Archipelago on the Coastal Scotian Shelf. *Journal of Geophysical Research. Oceans*, 127(3). <https://doi.org/10.1029/2021JC017791>
- 495
- Fennel, K., Alin, S., Barbero, L., Evans, W., Bourgeois, T., Cooley, S., Dunne, J., Feely, R. A., Hernandez-Ayon, J. M., Hu, X., Lohrenz, S., Muller-Karger, F., Najjar, R., Robbins, L., Shadwick, E., Siedlecki, S., Steiner, N., Sutton, A., Turk, D., ... Wang, Z. A. (2019). Carbon cycling in the North American coastal ocean: A synthesis. *Biogeosciences*, 16(6), 1281–1304. <https://doi.org/10.5194/bg-16-1281-2019>
- 500
- Fourqurean, J. W., Duarte, C. M., Kennedy, H., Marbà, N., Holmer, M., Mateo, M. A., Apostolaki, E. T., Kendrick, G. A., Krause-Jensen, D., McGlathery, K. J., & Serrano, O. (2012). Seagrass ecosystems as a globally significant carbon stock. *Nature Geoscience*, 5(7), 505–509. <https://doi.org/10.1038/ngeo1477>



- Giustini, F., Ciotoli, G., Rinaldini, A., Ruggiero, L., & Voltaggio, M. (2019). Mapping the geogenic radon potential and radon risk by using Empirical Bayesian Kriging regression: A case study from a volcanic area of central Italy. *The Science of the Total Environment*, 661, 449–464. <https://doi.org/10.1016/j.scitotenv.2019.01.146>
- 505
- Haar, C.D., Misiuk, B., Gazzola, V., Wells, M., Brown, C.J. (2023). Harmonizing multi-source backscatter data to generate regional seabed maps: Bay of Fundy, Canada. *Journal of Maps*, 19 (1) [doi.10.1080/17445647.2023.222362](https://doi.org/10.1080/17445647.2023.222362)
- Hedges, J. I., & Keil, R. G. (1995). Sedimentary organic matter preservation: An assessment and speculative synthesis. *Marine Chemistry*.
- 510
- Hilborn, R., Amoroso, R., Collie, J., Hiddink, J. G., Kaiser, M. J., Mazor, T., McConnaughey, R. A., Parma, A. M., Pitcher, C. R., Sciberras, M., & Suuronen, P. (2023). Evaluating the sustainability and environmental impacts of trawling compared to other food production systems. *ICES Journal of Marine Science*, fsad115. <https://doi.org/10.1093/icesjms/fsad115>
- 515
- Hilmi, N., Chami, R., Sutherland, M. D., Hall-Spencer, J. M., Lebleu, L., Benitez, M. B., & Levin, L. A. (2021). The Role of Blue Carbon in Climate Change Mitigation and Carbon Stock Conservation. *Frontiers in Climate*, 3, 710546. <https://doi.org/10.3389/fclim.2021.710546>
- Huang, Z., Nichol, S. L., Siwabessy, J. P., Daniell, J., & Brooke, B. P. (2012). Predictive modelling of seabed sediment parameters using multibeam acoustic data: a case study on the Carnarvon Shelf, Western Australia. *International Journal of Geographical Information Science*, 26(2), 283-307.
- 520
- Hunt, C. A., Demšar, U., Marchant, B., Dove, D., & Austin, W. E. N. (2021). Sounding Out the Carbon: The Potential of Acoustic Backscatter Data to Yield Improved Spatial Predictions of Organic Carbon in Marine Sediments. *Frontiers in Marine Science*, 8, 756400. <https://doi.org/10.3389/fmars.2021.756400>
- Hunt, C., Demšar, U., Dove, D., Smeaton, C., Cooper, R., & Austin, W. E. N. (2020). Quantifying Marine Sedimentary Carbon: A New Spatial Analysis Approach Using Seafloor Acoustics, Imagery, and Ground-Truthing Data in Scotland. *Frontiers in Marine Science*, 7, 588. <https://doi.org/10.3389/fmars.2020.00588>
- 525
- Jeffery. (2020). *Biophysical and Ecological Overview of the Eastern Shore Islands Area of Interest (AOI)*.
- Jenkins C (2005) Summary of the on-CALCULATION methods used in dbSEABED. <http://pubs.usgs.gov/ds/2006/146/docs/onCALCULATION.pdf>. Accessed 27 July 2023



- 530 King, E. L. (2018). *Surficial geology and features of the inner shelf of eastern shore, offshore Nova Scotia* (8375; p. 8375). <https://doi.org/10.4095/308454>
- Legge, O., Johnson, M., Hicks, N., Jickells, T., Diesing, M., Aldridge, J., Andrews, J., Artioli, Y., Bakker, D. C. E., Burrows, M. T., Carr, N., Cripps, G., Felgate, S. L., Fernand, L., Greenwood, N., Hartman, S., Kröger, S., Lessin, G., Mahaffey, C., ... Williamson, P. (2020). Carbon on the Northwest European Shelf: Contemporary Budget and Future Influences. *Frontiers in Marine Science*, 7, 143. <https://doi.org/10.3389/fmars.2020.00143>
- Liaw, A., Wiener, M., 2002. Classification and regression by randomForest. *R news* 2, 18–22.
- Lucieer, V., Hill, N. A., Barrett, N. S., & Nichol, S. (2013). Do marine substrates ‘look’ and ‘sound’ the same? Supervised classification of multibeam acoustic data using autonomous underwater vehicle images. *Estuarine, Coastal and Shelf Science*, 117, 94–106.
- 540 Mallik, S., Bhowmik, T., Mishra, U., & Paul, N. (2022). Mapping and prediction of soil organic carbon by an advanced geostatistical technique using remote sensing and terrain data. *Geocarto International*, 37(8), 2198–2214. <https://doi.org/10.1080/10106049.2020.1815864>
- Mason C. 2011. NMBAQC’s Best Practice Guidance. Particle Size Analysis (PSA) for Supporting Biological Analysis. National Marine Biological AQC Coordinating Committee.
- 545 Mayer, L., Jakobsson, M., Allen, G., Dorschel, B., Falconer, R., Ferrini, V., Lamarche, G., Snaith, H., Weatherall, P. (2018). The Nippon Foundation—GEBSCO Seabed 2030 Project: The Quest to See the World’s Oceans Completely Mapped by 2030. *Geosciences*. 8(2):63. doi:10.3390/geosciences8020063.
- Mayr, F. B., Upton, H. F. (Harold F., Buck, E. H., Upton, H. F. (Harold F., & Vann, A. (2010). *Marine protected areas*. 550 Nova Science Publishers.
- Misiuk, B., Brown, C.J. (2023) Benthic habitat mapping: A review of three decades of mapping biological patterns on the seafloor. *Estuarine Coastal and Shelf Science*. In Press
- Misiuk, B., Brown, C.J., Robert, K., Lacharite, M. (2020). Harmonizing multi-source sonar backscatter datasets for seabed mapping using bulk shift approaches. *Remote Sensing*. 12(4): 601. <https://doi.org/10.3390/rs12040601>
- 555



- Misiuk, B., Diesing, M., Aitken, A., Brown, C. J., Edinger, E. N., & Bell, T. (2019). A spatially explicit comparison of quantitative and categorical modelling approaches for mapping seabed sediments using random forest. *Geosciences (Basel)*, 9(6), 254–. <https://doi.org/10.3390/geosciences9060254>
- 560 Misiuk, B., Lacharité, M., Brown, C.J. (2021). Assessing the use of harmonized multisource backscatter data for thematic benthic habitat mapping. *Science of Remote Sensing*. 3. doi.10.1016/j.srs.2021.1000
- Mitchell, P. J., Aldridge, J., & Diesing, M. (2019). Legacy data: How decades of seabed sampling can produce robust predictions and versatile products. *Geosciences (Basel)*, 9(4), 182–. <https://doi.org/10.3390/geosciences9040182>
- Mollenhauer G, Schneider RR, Jennerjahn T et al (2004) Organic carbon accumulation in the South Atlantic Ocean: 565 its modern, mid-Holocene and last glacial distribution. *Glob Planet C*
- Najjar, R. G., Herrmann, M., Alexander, R., Boyer, E. W., Burdige, D. J., Butman, D., Cai, W. -J., Canuel, E. A., Chen, R. F., Friedrichs, M. A. M., Feagin, R. A., Griffith, P. C., Hinson, A. L., Holmquist, J. R., Hu, X., Kemp, W. M., Kroeger, K. D., Mannino, A., McCallister, S. L., ... Zimmerman, R. C. (2018). Carbon Budget of Tidal Wetlands, Estuaries, and Shelf Waters of Eastern North America. *Global Biogeochemical Cycles*, 32(3), 389– 570 416. <https://doi.org/10.1002/2017GB005790>
- Sala, E., Mayorga, J., Bradley, D., Cabral, R. B., Atwood, T. B., Auber, A., Cheung, W., Costello, C., Ferretti, F., Friedlander, A. M., Gaines, S. D., Garilao, C., Goodell, W., Halpern, B. S., Hinson, A., Kaschner, K., Kesner-Reyes, K., Leprieux, F., McGowan, J., ... Lubchenco, J. (2021). Protecting the global ocean for biodiversity, food and climate. *Nature*, 592(7854), 397–402. <https://doi.org/10.1038/s41586-021-03371-z>
- 575 Simons, D. G., & Snellen, M. (2009). A Bayesian approach to seafloor classification using multi-beam echo-sounder backscatter data. *Applied Acoustics*, 70(10), 1258-1268.
- Smeaton, C., & Austin, W. E. N. (2019). Where's the Carbon: Exploring the Spatial Heterogeneity of Sedimentary Carbon in Mid-Latitude Fjords. *Frontiers in Earth Science*, 7, 269. <https://doi.org/10.3389/feart.2019.00269>
- Smeaton, C., Yang, H., & Austin, W. E. N. (2021). Carbon burial in the mid-latitude fjords of Scotland. *Marine Geology*, 441, 106618. <https://doi.org/10.1016/j.margeo.2021.106618>
- 580 Snelgrove, P. V. R., Soetaert, K., Solan, M., Thrush, S., Wei, C.-L., Danovaro, R., Fulweiler, R. W., Kitazato, H., Ingole, B., Norkko, A., Parkes, R. J., & Volkenborn, N. (2018). Global Carbon Cycling on a Heterogeneous Seafloor. *Trends in Ecology & Evolution*, 33(2), 96–105. <https://doi.org/10.1016/j.tree.2017.11.004>





Sokal RR, Rohlf FJ (1981) Biometry. San Francisco, USA

585 Stephens, D., & Diesing, M. (2014). A comparison of supervised classification methods for the prediction of substrate  
type using multibeam acoustic and legacy grain-size data. *PloS one*, 9(4), e93950.

Stephens, D., & Diesing, M. (2015). Towards quantitative spatial models of seabed sediment composition. *PloS One*,  
10(11), e0142502–e0142502. <https://doi.org/10.1371/journal.pone.0142502>

Vandermeulen, H. (2018). *A Drop Camera Survey of the Eastern Shore Archipelago, Nova Scotia*. Canadian Technical  
590 Report of Fisheries and Aquatic Sciences 3258. [https://publications.gc.ca/collections/collection\\_2018/mpo-  
dfo/Fs97-6-3258-eng.pdf](https://publications.gc.ca/collections/collection_2018/mpo-dfo/Fs97-6-3258-eng.pdf)

Verardo, D. J., Froelich, P. N., & McIntyre, A. (1990). Determination of organic carbon and nitrogen in marine  
sediments using the Carlo Erba NA-1500 analyzer. *Deep Sea Research Part A. Oceanographic Research  
Papers*, 37(1), 157–165. [https://doi.org/10.1016/01980149\(90\)90034-S](https://doi.org/10.1016/01980149(90)90034-S)

595